



GTC-OSIRIS, tunable filters, and LAE/LBG candidate detection

Mario Andrés De Leo Winkler

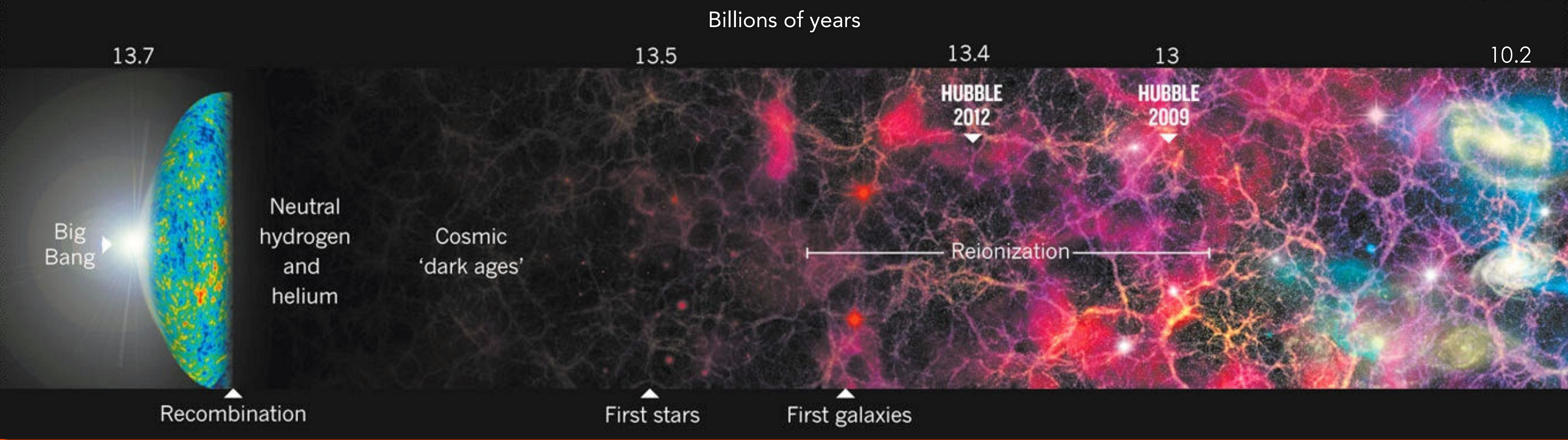
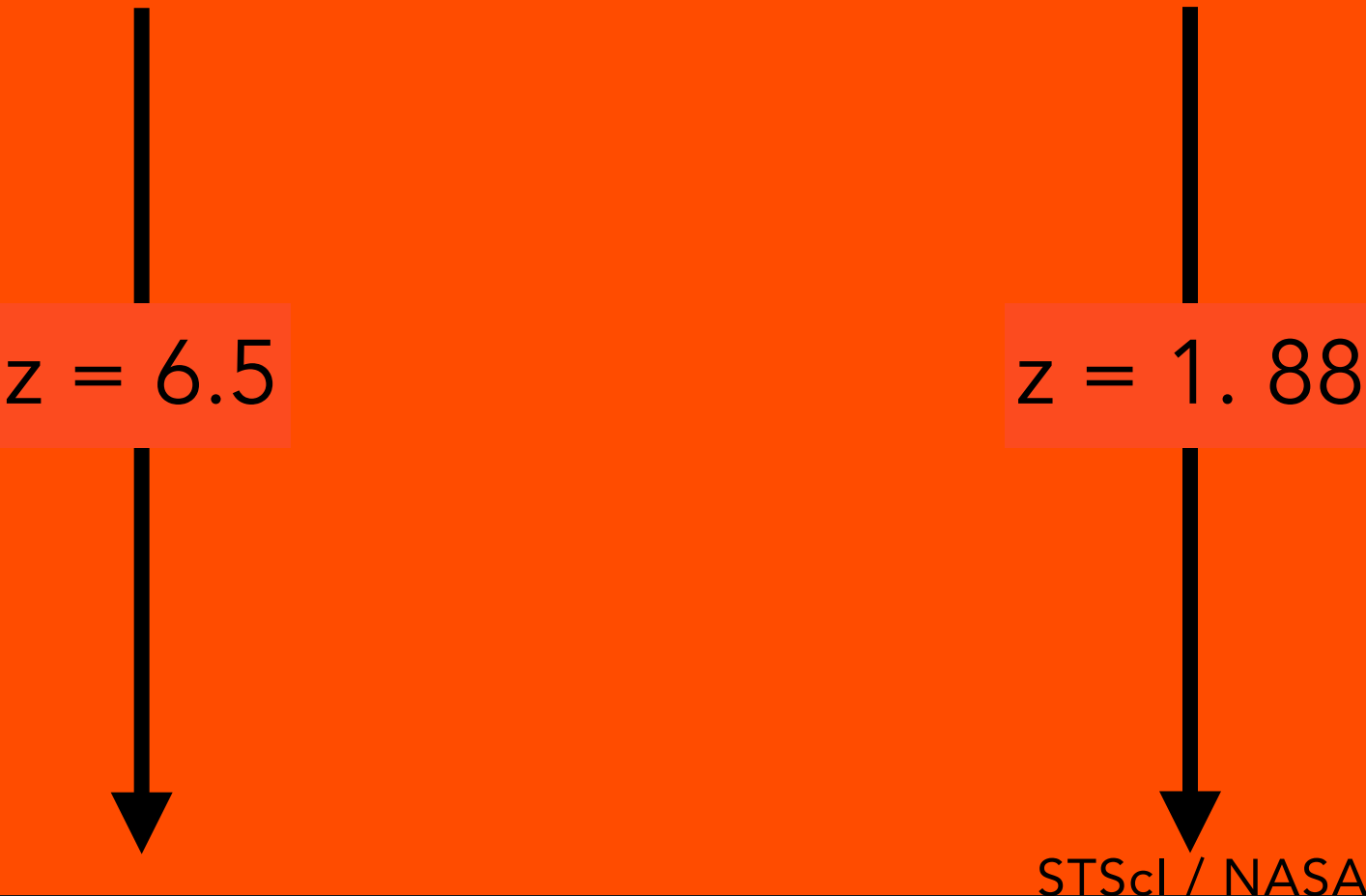
de Diego, J.A., Cepa, J., Bongiovanni, A., Verdugo, T., Sánchez-Portal., M., González-Serrano, J.I.

Instituto de Astronomía UNAM, Mexico - IAC, Spain - CIDA, Venezuela

What is it good for?

Understand:

- end of ionization
- chemical evolution
- evolution of dust
- morphological evolution of galaxies
- stellar formation
- spatial grouping



de Diego, De Leo, et al., 2013, AJ, 146 published

Why?

Based on 2 successful methods on their respective fields (TF at low redshift and Lyman Alpha emitter detection in wide filters) joined for high-redshift search

Pilot program of OSIRIS-TF (tunable filters) photometric data to look for LAEs

TFs allow for a maximum signal-to-noise ratio

Obtain characteristics of LAEs during the end of the re-ionization period

Gives very good photometric redshift estimation of candidate emitters

We are not sure on the intrinsic difference (if there exists) between LAEs & LBGs

Data

3 galaxy clusters (MS2053, MS0440, MS1358)
with strong gravitation lensing
& detailed mass models

Verdugo, et al., 2008, ApJ, 664

$\sim 6800 \text{ \AA}$ ($z \sim 4.6$)

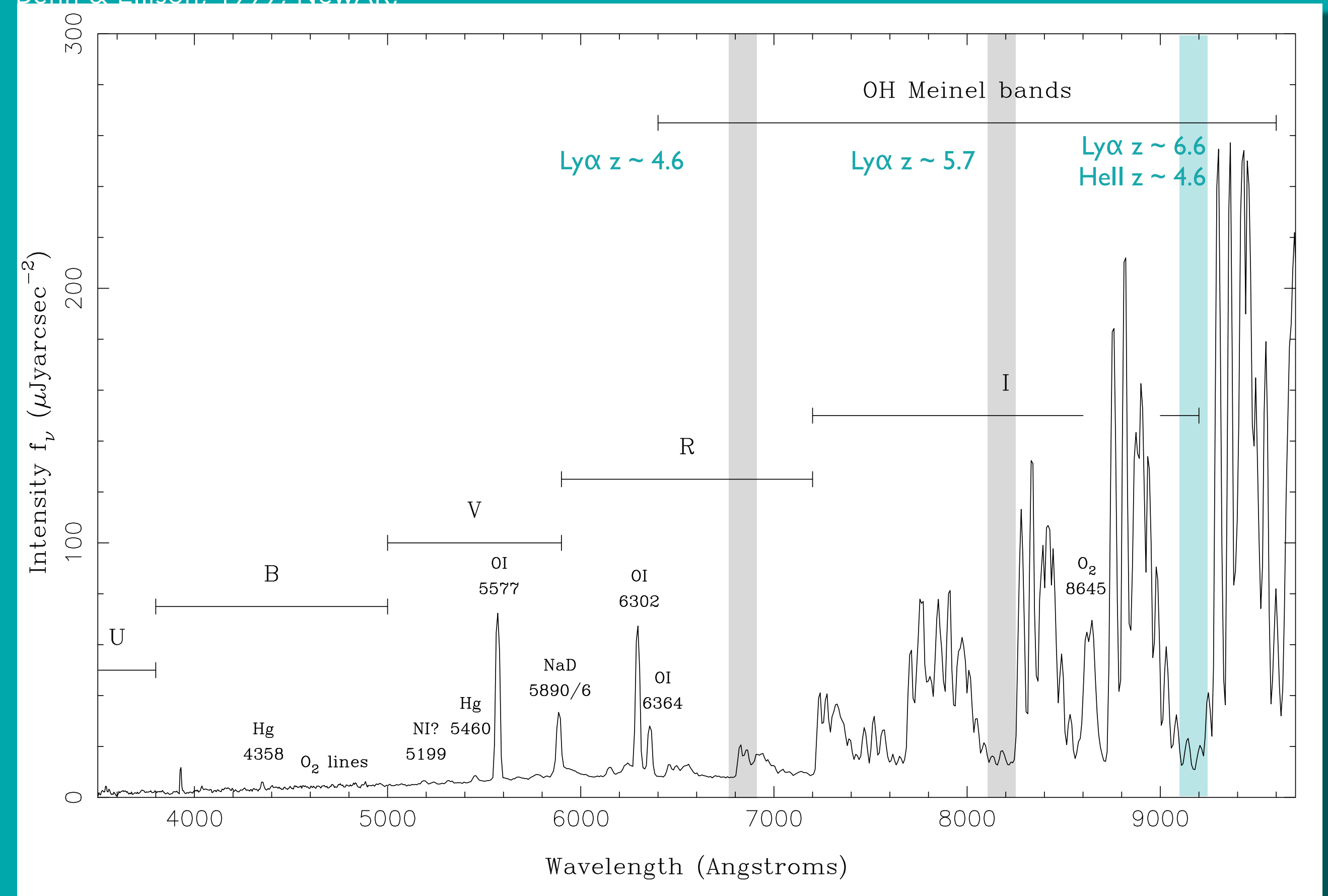
$\sim 8150 \text{ \AA}$ ($z \sim 5.7$)

$\sim 9100 \text{ \AA}$ ($z \sim 6.6$)

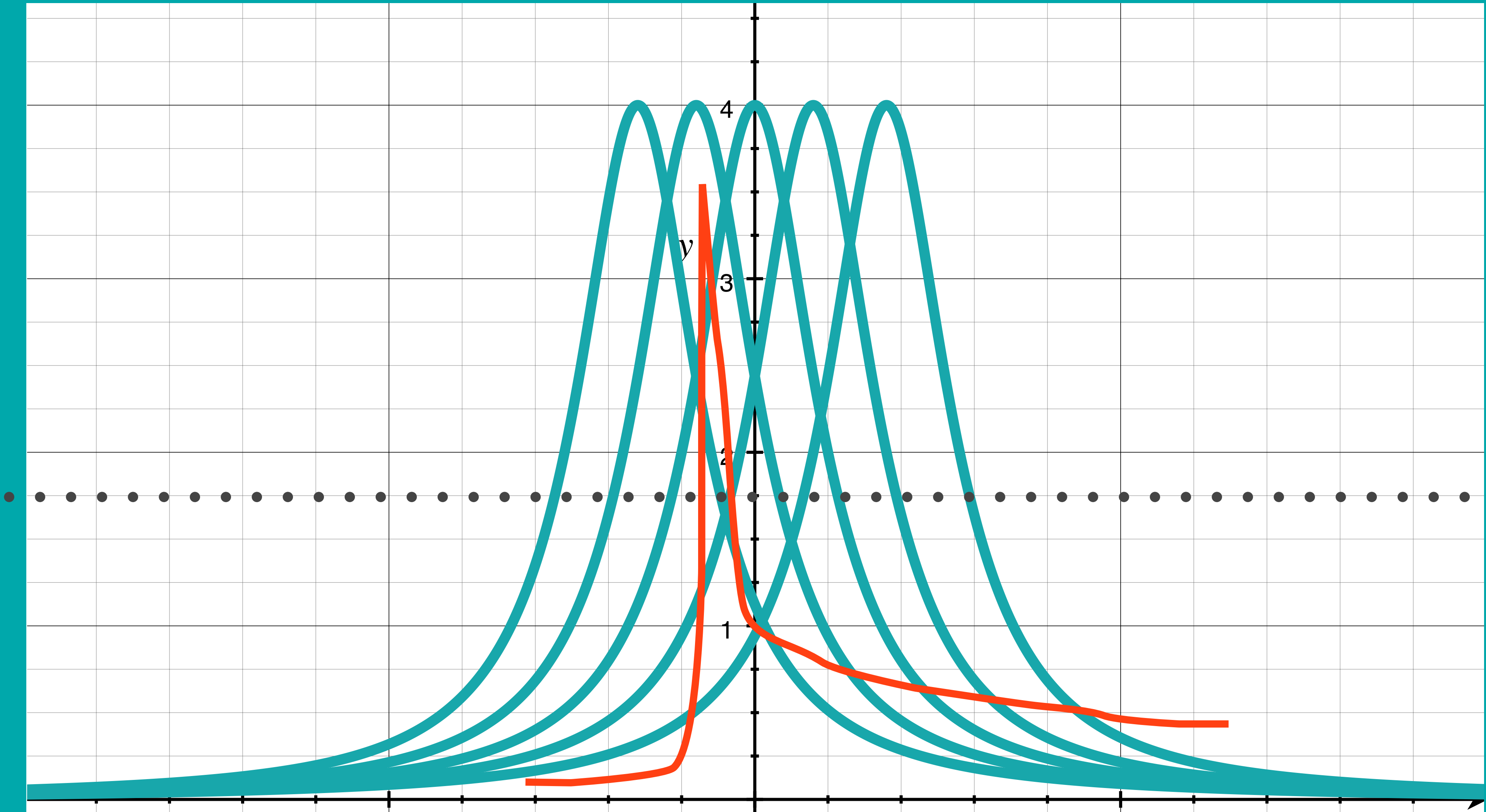
regions without strong sky emission
dual emitters Ly α - HeII (1640 \AA)

Nagao, et al., 2008, ApJ, 680

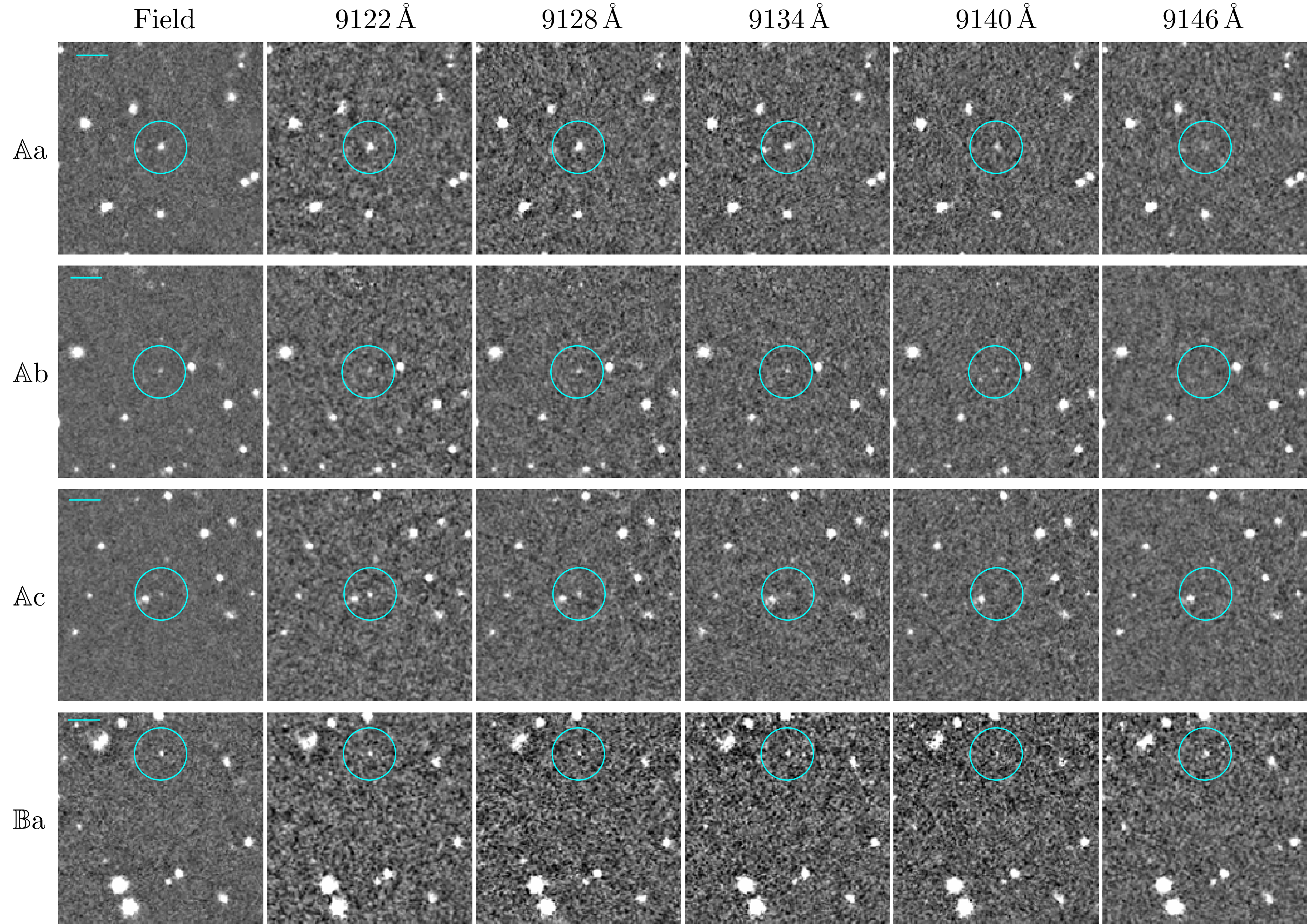
Benn & Ellison, 1999, NewAR.



Method



Candidates



Candidates

Only in MS2053

Only in 5 wavelengths

< 0.82" seeing

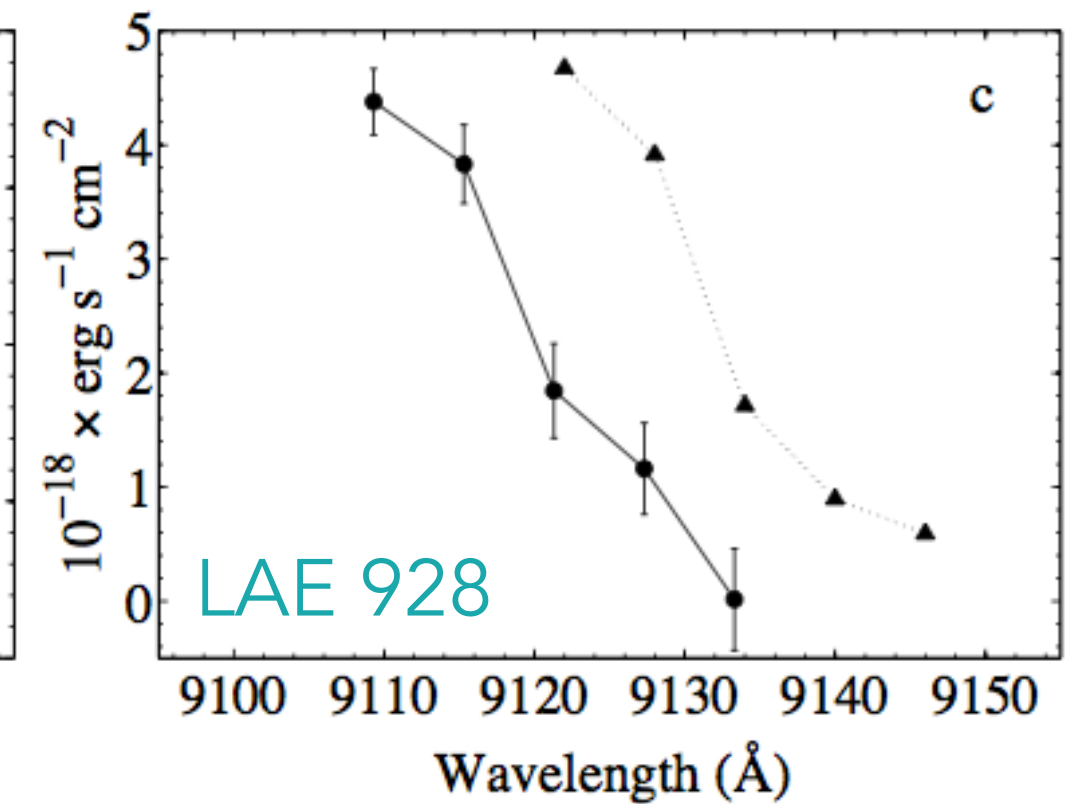
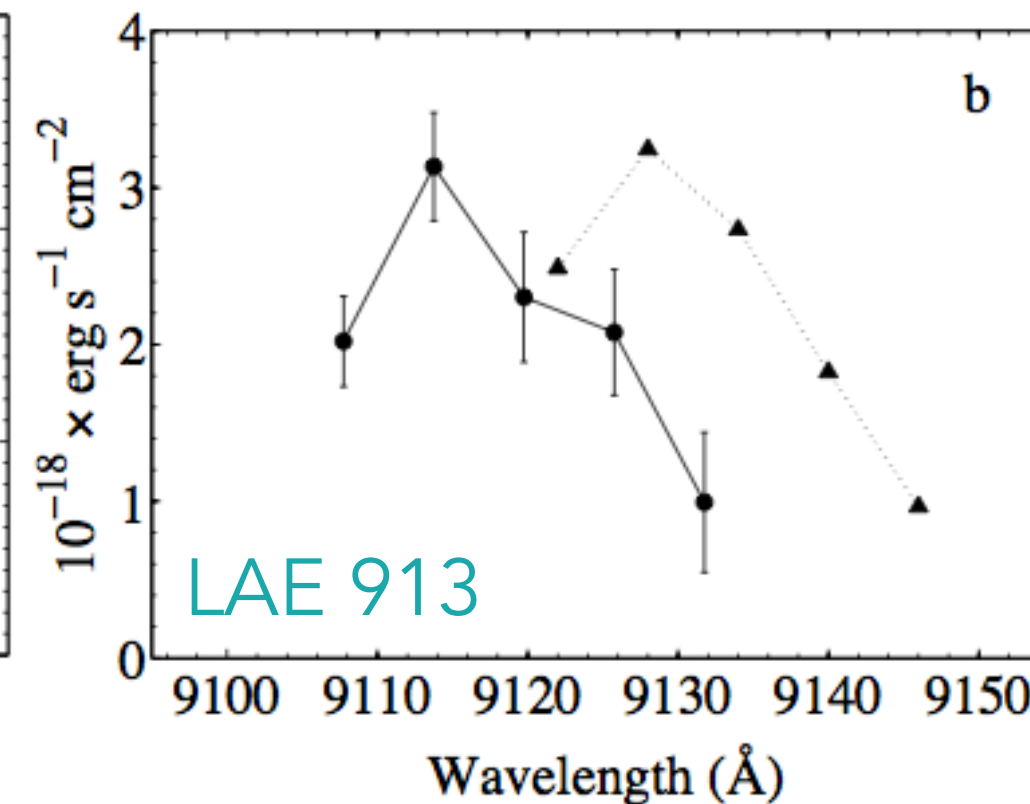
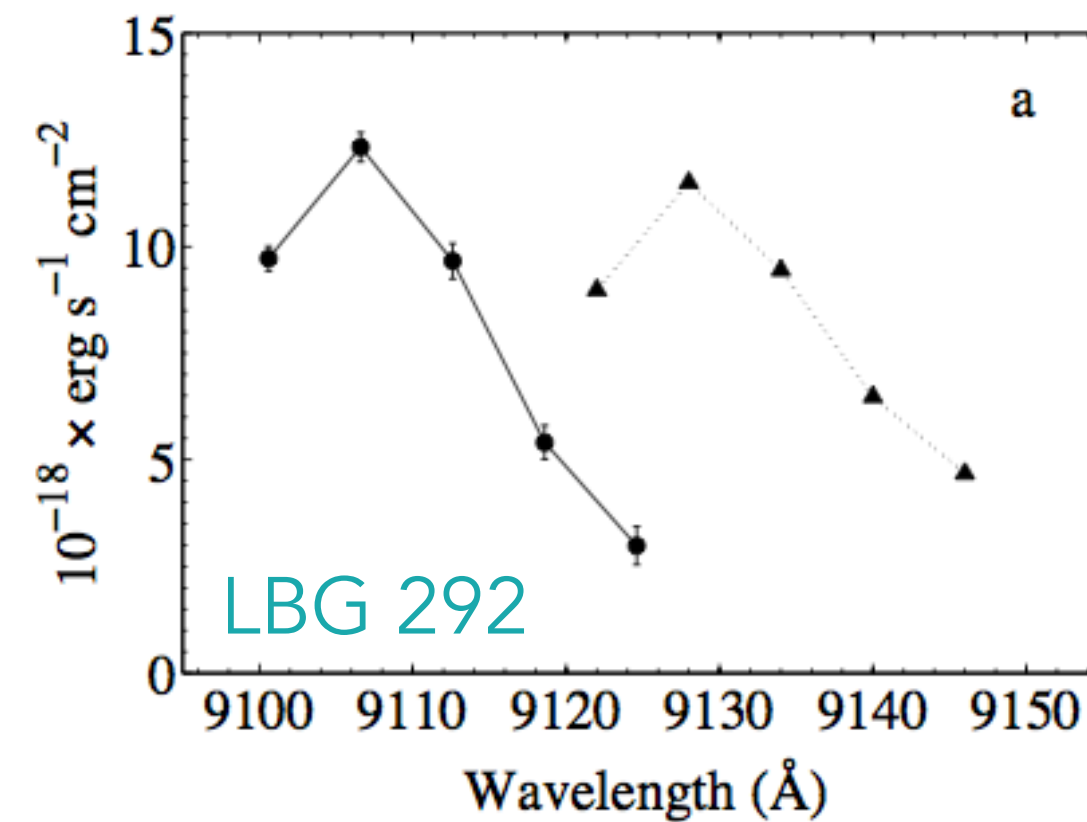
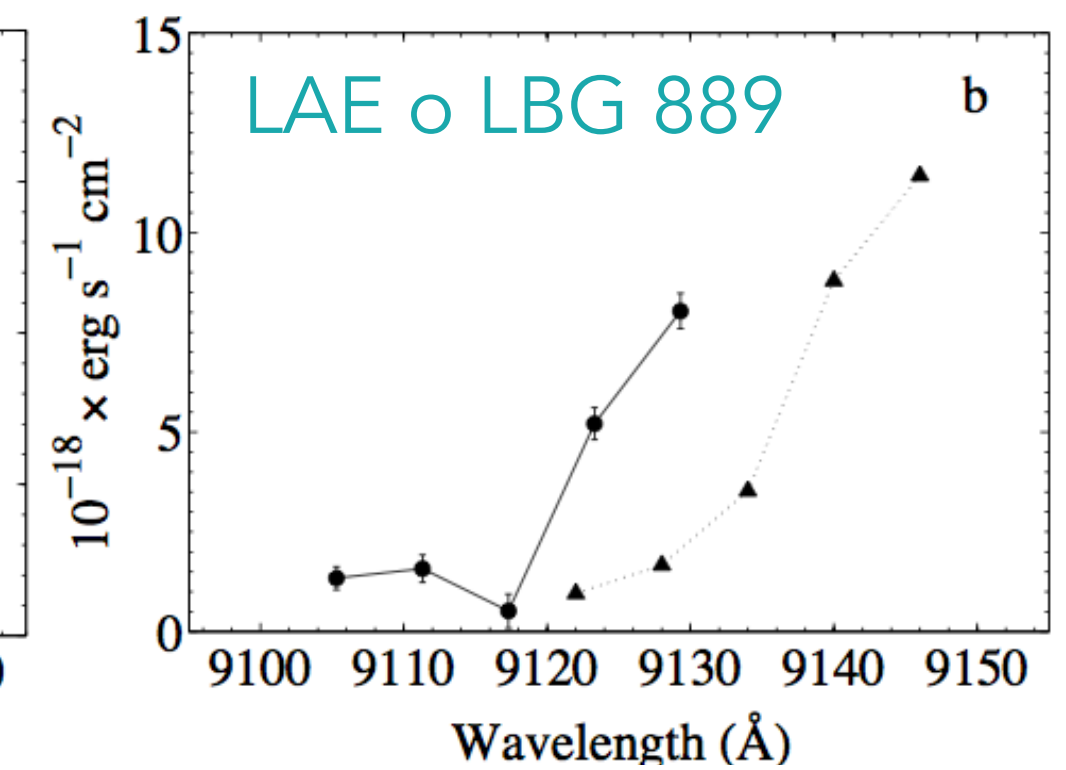
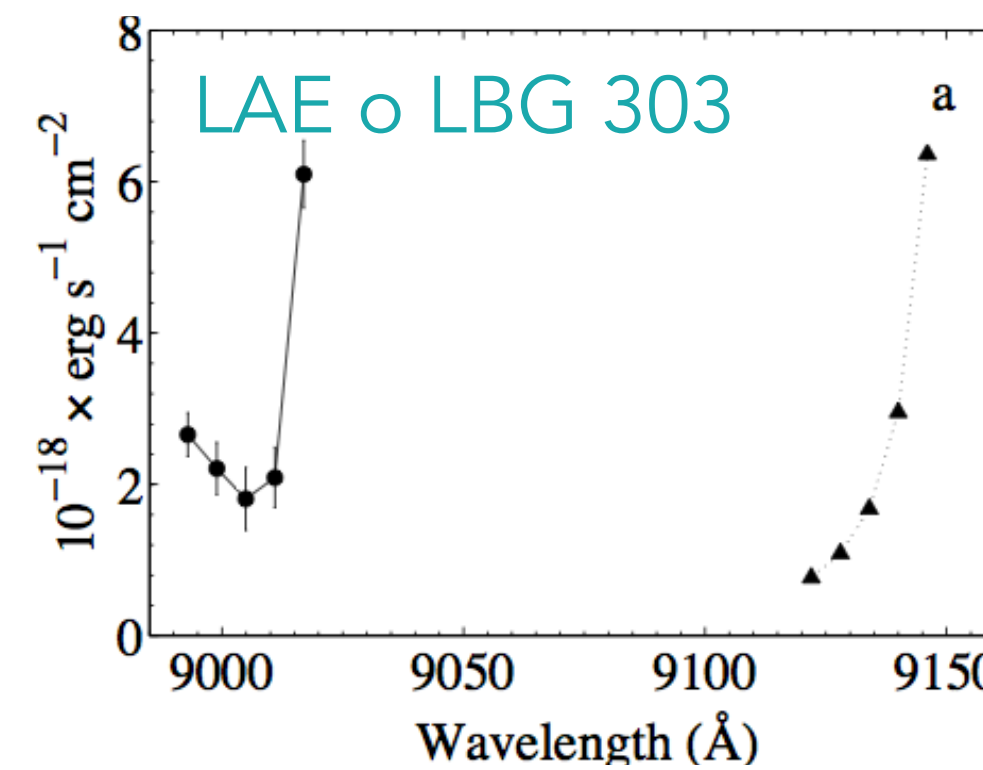
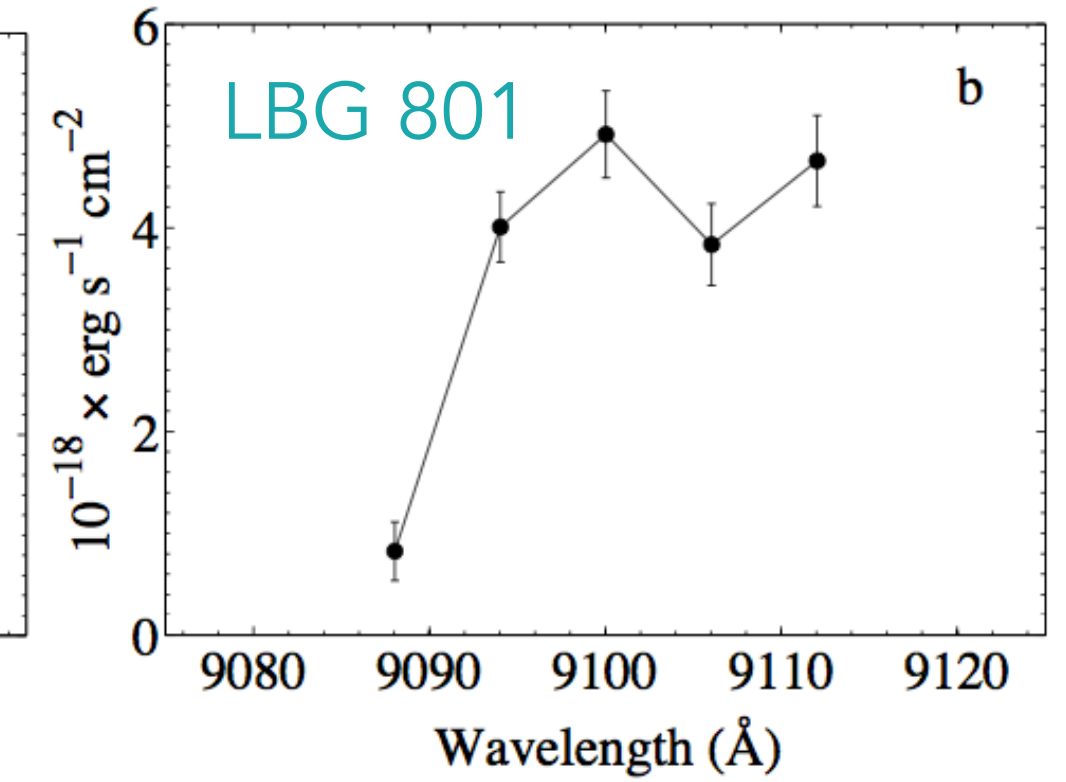
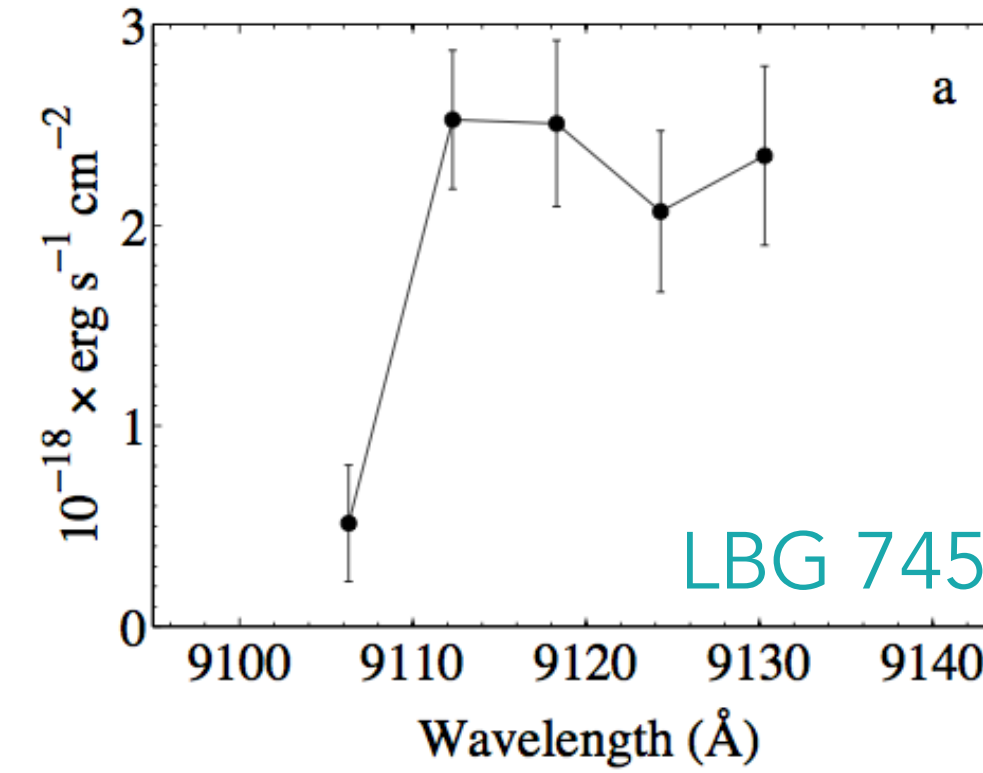
5 contiguous filters

Similar simulations, not adjusted in flux

Observations



Simulations



Candidates

Table 2
Candidate Fluxes

| Filter | Aa | Ab | Ac | Ba | Bb | Ca | Cb |
|-------------------|-------------|--------------|-------------|-------------|-------------|-------------|-------------|
| Suprime <i>V</i> | 26 ± 2 | <0.70 | 4 ± 1 | 8.3 ± 0.7 | ... | 36 ± 1 | ... |
| F606W | ... | ... | ... | ... | ... | 41 ± 7 | ... |
| F702W | ... | ... | 1.5 ± 0.2 | ... | ... | ... | ... |
| Suprime <i>i'</i> | 7.3 ± 0.3 | 7.5 ± 0.2 | 1.3 ± 0.1 | 11.0 ± 0.3 | 4.0 ± 0.2 | ... | 9.7 ± 0.2 |
| F814W | ... | ... | 0.5 ± 0.2 | ... | ... | 9.0 ± 0.6 | ... |
| OSIRIS-TF | 38 ± 1 | 18 ± 2 | 10 ± 1 | 22 ± 2 | 12.0 ± 0.8 | 15 ± 1 | 20.9 ± 0.3 |
| Suprime <i>z'</i> | 7.3 ± 0.4 | 21.0 ± 0.6 | 0.7 ± 0.4 | 16 ± 2 | 4.0 ± 0.4 | ... | 17.0 ± 0.3 |
| 3.6 μm | 0.55 ± 0.03 | 10.34 ± 0.04 | <0.15 | 0.41 ± 0.06 | <0.15 | 1.86 ± 0.03 | 0.44 ± 0.02 |
| 4.5 μm | 0.47 ± 0.03 | 6.37 ± 0.03 | <0.08 | <0.08 | <0.08 | 1.15 ± 0.03 | 0.24 ± 0.03 |
| 5.8 μm | 0.80 ± 0.07 | 3.47 ± 0.07 | 0.69 ± 0.07 | <0.14 | <0.14 | 0.77 ± 0.07 | 0.36 ± 0.07 |
| 8.0 μm | <0.17 | 1.73 ± 0.08 | <0.17 | <0.17 | 0.44 ± 0.09 | <0.17 | <0.17 |

Note. All the fluxes in units of 10^{-19} erg s⁻¹ cm⁻² Å⁻¹.

SED fitting

HyperZ

Bolzonella, et al., 2000, A&A, 363

Filters used:

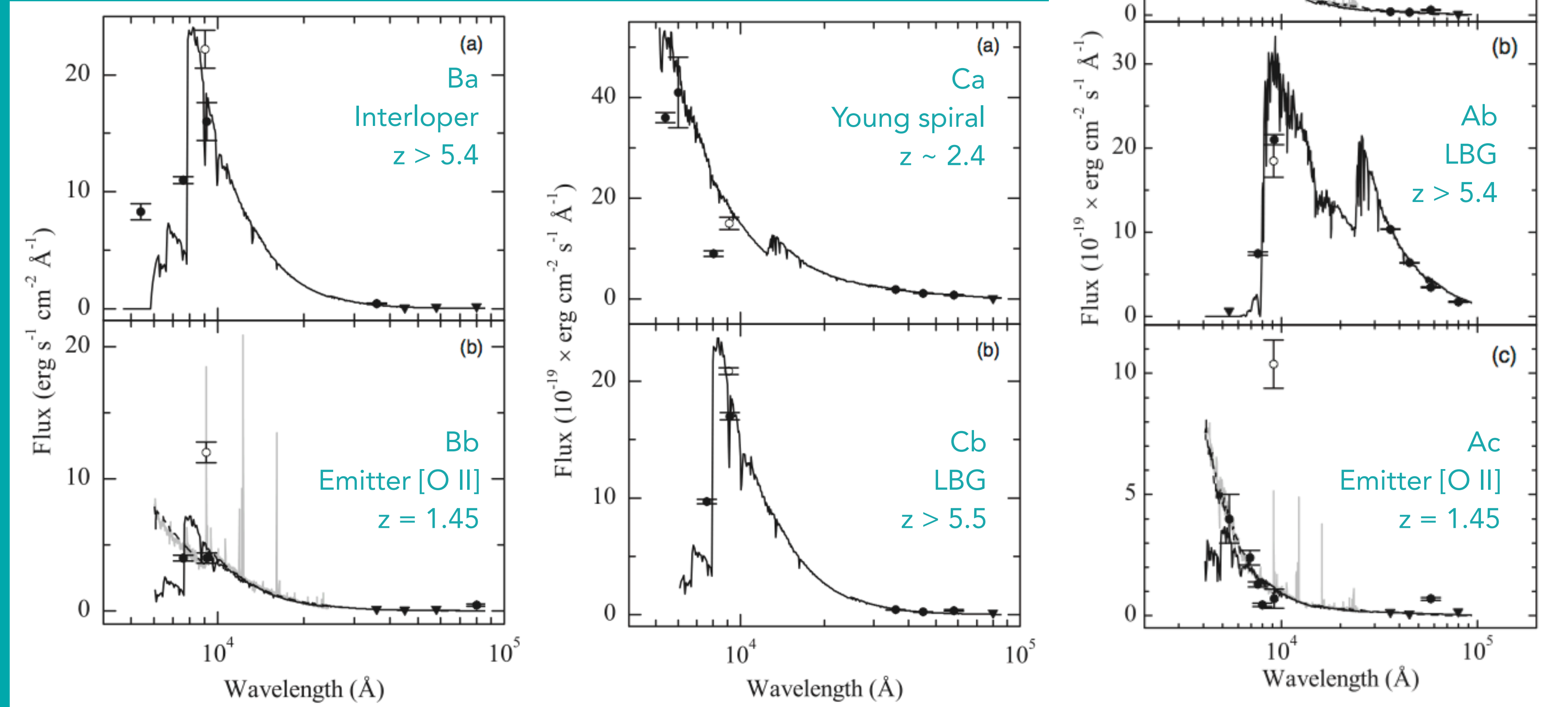
4 Spitzer/IRAC +

3 HST/WFPC2 F606,702,814W +

Subaru Suprime Cam z'

Hollow circles are OSIRIS data

Gray line shows fit for interloper emitter [O II]_{3726-9 Å}



Simulations

5000 simulated LAEs

OSIRIS - TFs have Lorentzian profile

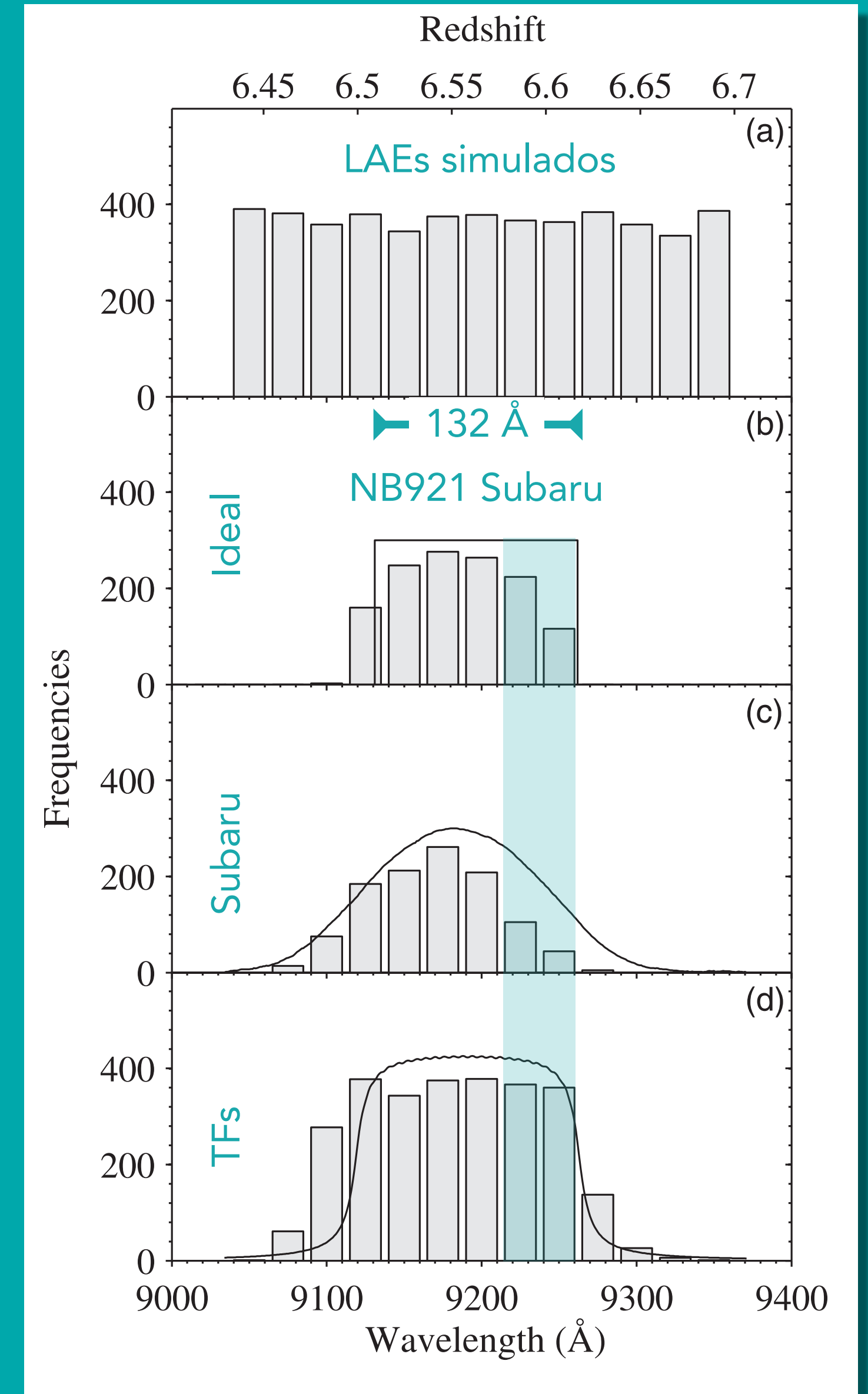
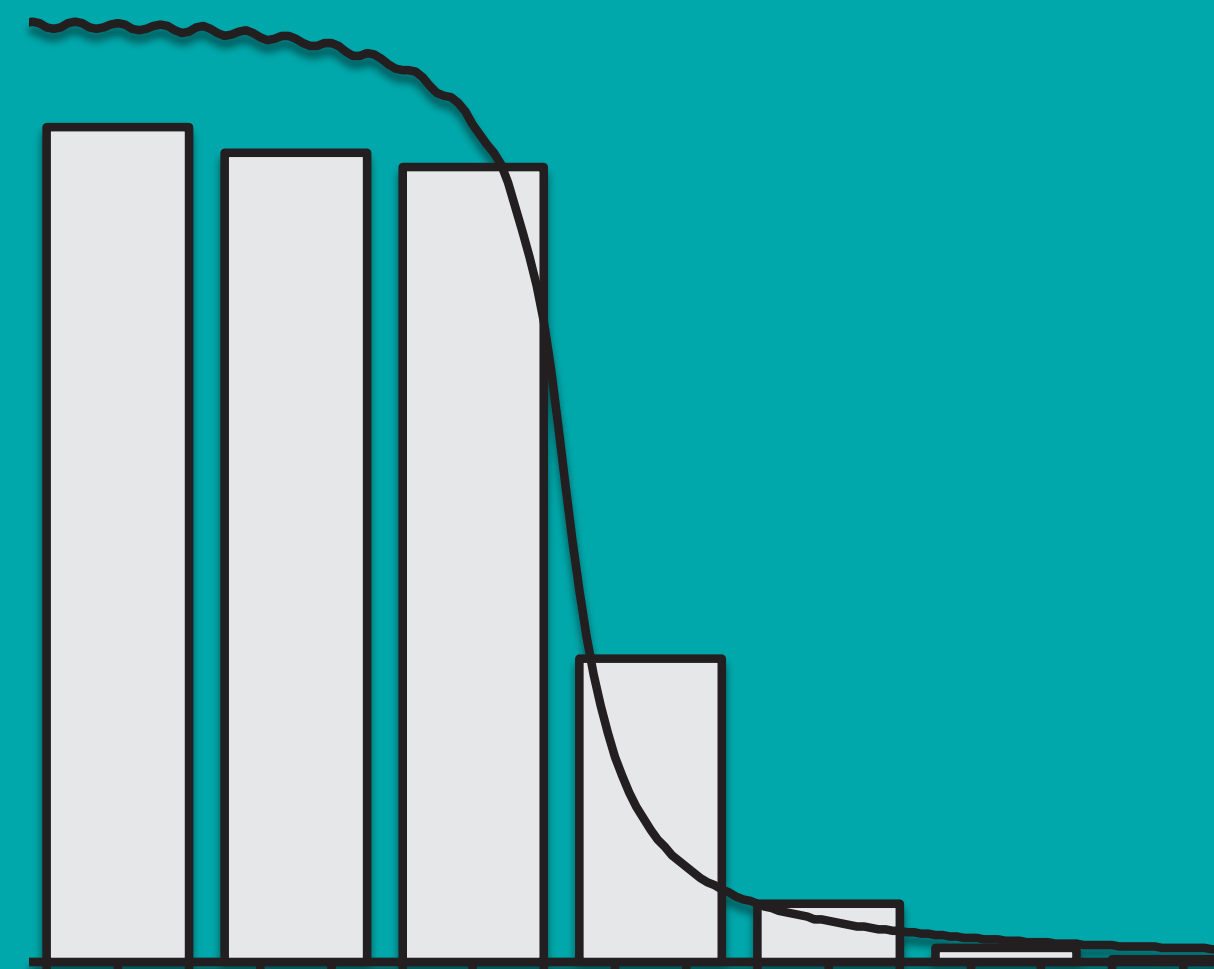
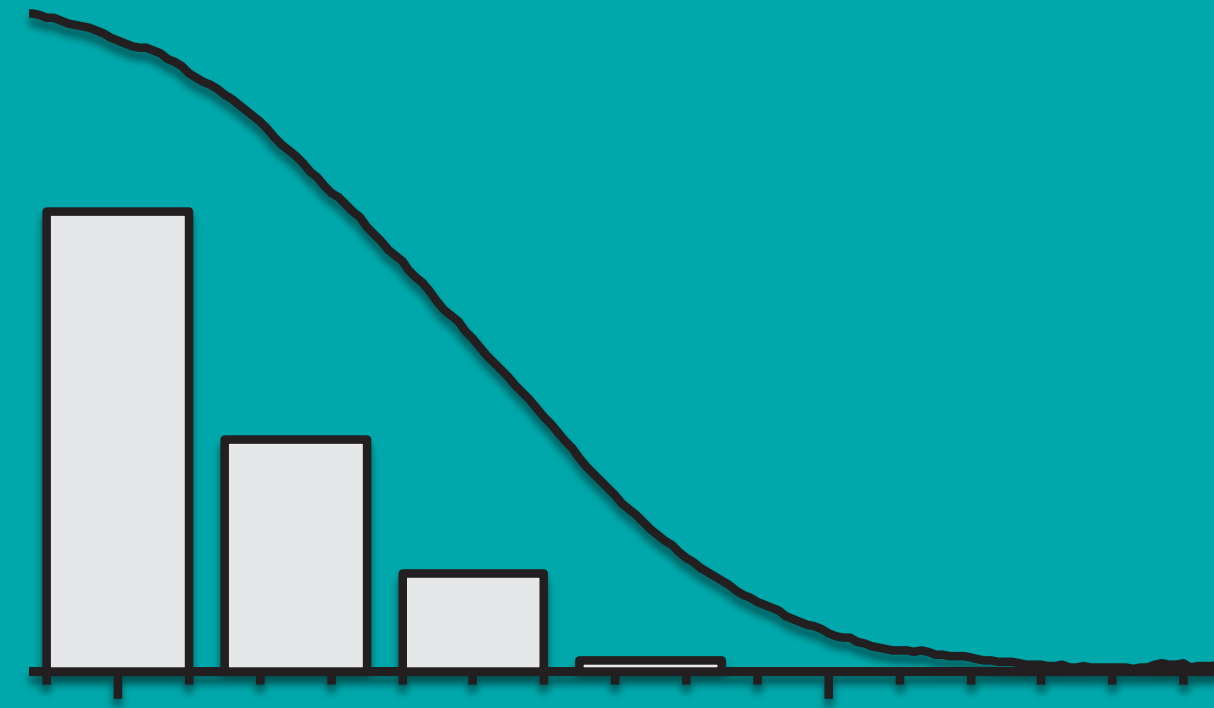
Preserves Ly α 's asymmetric profile in pseudo-spectra

$I_{\text{rr}} \geq 9 \times 10^{-18} \text{ erg s}^{-1} \text{ cm}^{-2} \text{ (frame)}$

1 magnitude of difference for detection

Similar to detection method by

Ouchi, et al., 2010, ApJ, 723

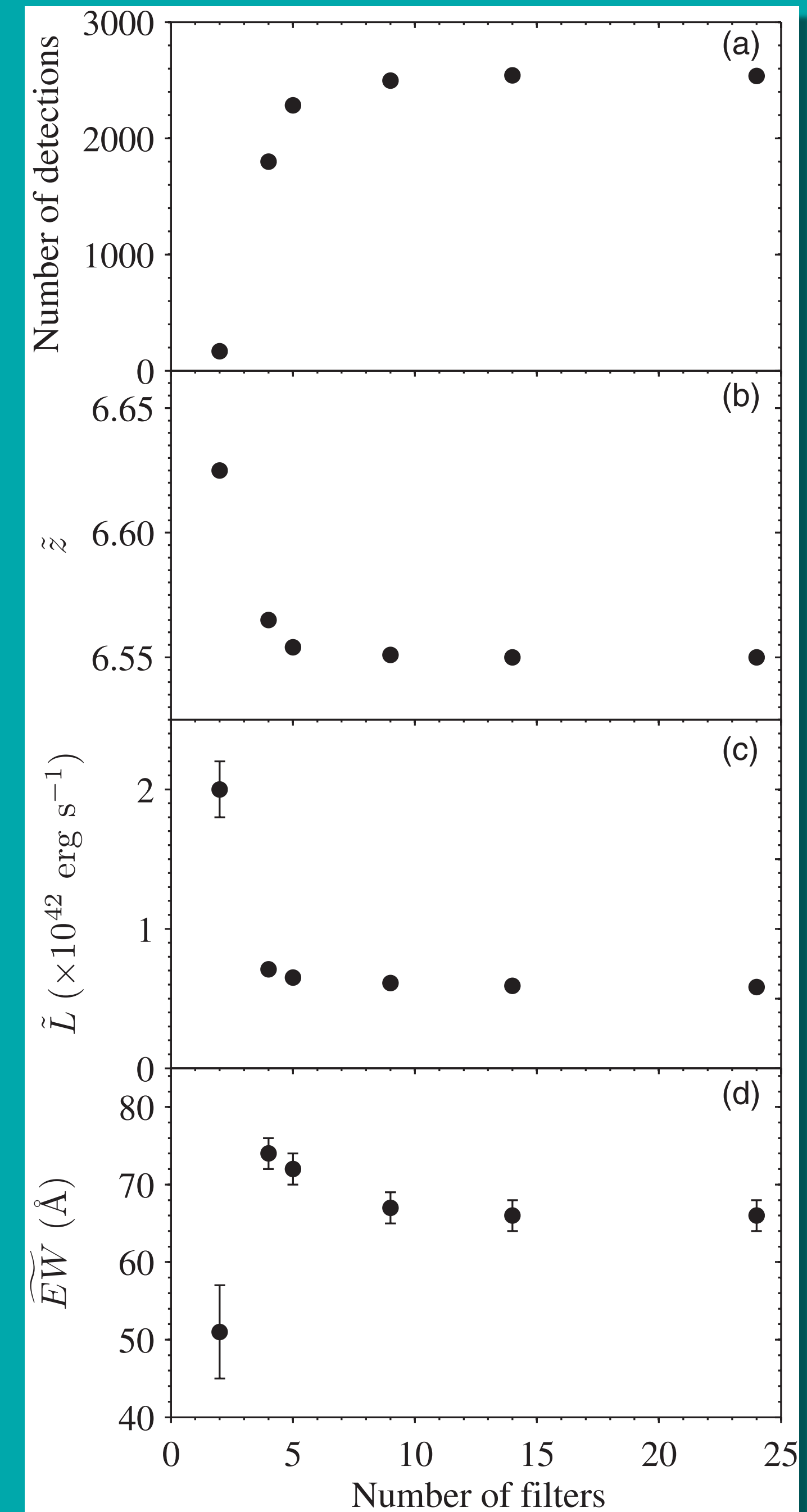


Simulations

2500 objects

Strongly decays with 2 filters

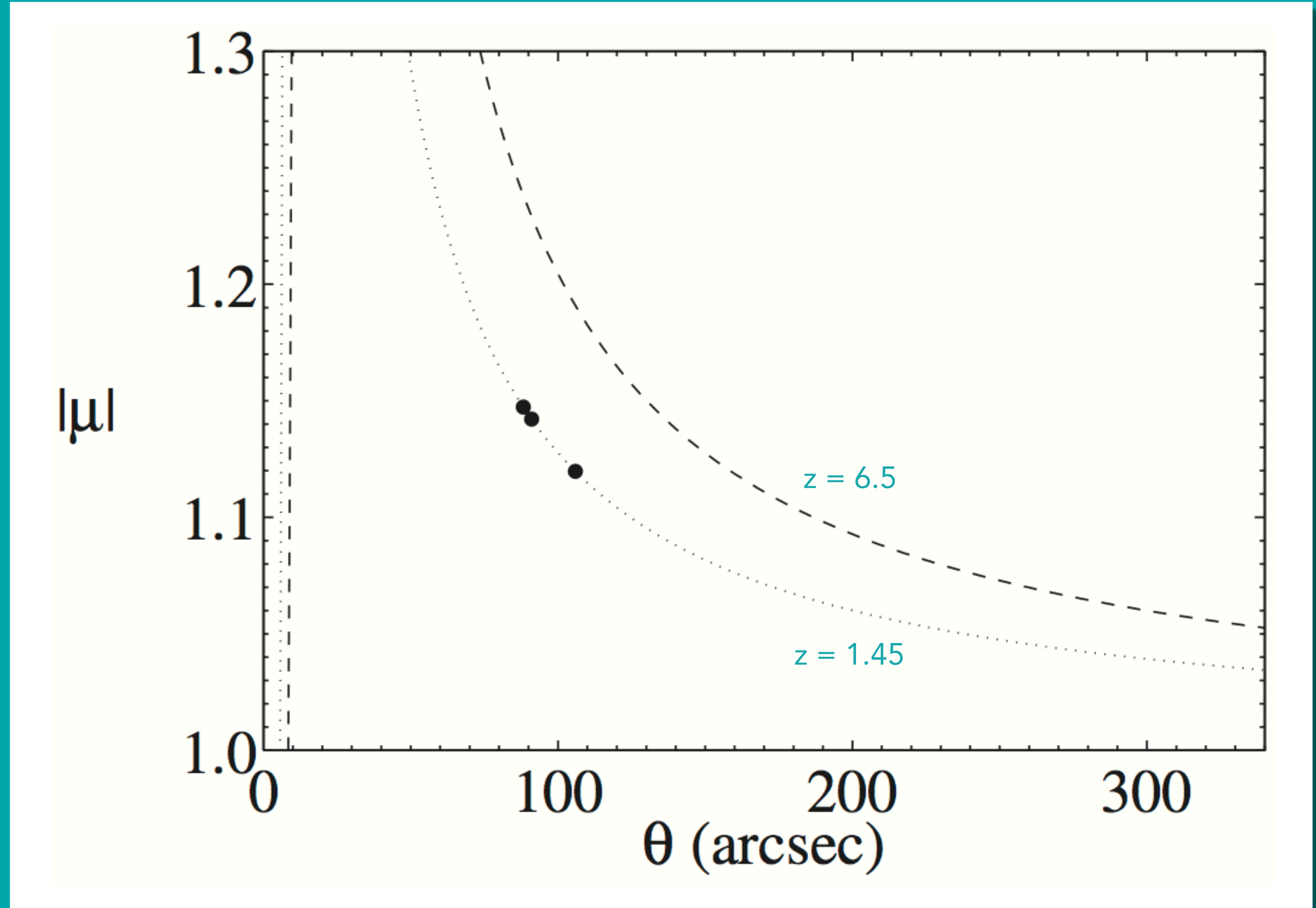
Reaches an optimum number at 9 filters



Magnification

LENSTOOL

Jullo, et al., 2007, NJP, 9



Simulations

Table 6
OSIRIS-TF Survey Expected Quantities

| Parameter | Observations ^a | |
|--|---------------------------|---------|
| | Planned | Accomp. |
| Slices ^b | 24 | 5 |
| Irradiance limit ^c | 4 | 9 |
| $L_{\text{Ly}\alpha}$ limit ^d | 2.1 | 4.7 |
| Volume LAEs ^e | 8760 | 1503 |
| Expected LAEs ^f | 4.2 | 0.1 |
| $L_{[\text{O II}]}$ limit ^g | 2.9 | 6.4 |
| Volume [O II] ^e | 122 | 21 |
| Expected [O II] (Takahashi) ^h | 7.4 | 0.8 |
| Expected [O II] (Dressler) ⁱ | 2.5 | 0.2 |

Notes.

^a State of the observations: Planned or Accomplished.

^b Number of wavelength slices.

^c Irradiance lower limit ($\times 10^{-18}$ erg s⁻¹ cm⁻²).

^d Ly α luminosity lower limit ($\times 10^{42}$ erg s⁻¹).

^e Proper volume covered (Mpc⁻³).

^f Number of expected LAEs obtained through the Schechter function with Kashikawa et al. (2011) parameters. Numbers are given with a precision of one decimal place, rather than integers, to ensure that at least one significant digit is shown.

^g [O II] luminosity lower limit ($\times 10^{40}$ erg s⁻¹).

^h Takahashi et al. (2007).

ⁱ Dressler et al. (2011).

Conclusions

GTC-OSIRIS-TF

Good photometric redshift (10x spectral resolution than wide filters)

Detects Ly α lines with a smaller EW

Requires more observation time

Sweeps less covolume

SUBARU

Does not detect emitters with small EW

Does not reproduce the asymmetric profile of the Ly α line

Rough redshift estimate

Sweeps more covolume

Both are complimentary strategies

Will benefit from EMIR observations